Wavelength-Converted/Selective Waveguiding Based on Composition-Graded Semiconductor Nanowires

ARTICLE *in* NANO LETTERS · AUGUST 2012

Impact Factor: 13.59 · DOI: 10.1021/nl302693c · Source: PubMed

14 AUTHORS, INCLUDING:

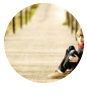

Wei Hu
Hunan University
17 PUBLICATIONS **184** CITATIONS
SEE PROFILE

Xiaoli Zhu
Hunan University
54 PUBLICATIONS **277** CITATIONS
SEE PROFILE

Limin Tong
Zhejiang University
188 PUBLICATIONS **5,013** CITATIONS
SEE PROFILE

Xiangfeng Duan
University of California, Los Angeles
173 PUBLICATIONS **18,058** CITATIONS
SEE PROFILE

NANO LETTERS

Letter

pubs.acs.org/NanoLett

Wavelength-Converted/Selective Waveguiding Based on Composition-Graded Semiconductor Nanowires

Jinyou Xu,[†,⊥] Xiujuan Zhuang,[†,⊥] Pengfei Guo,[†,⊥] Qinglin Zhang,[†] Weiqing Huang,[†] Qiang Wan,[†] Wei Hu,[†] Xiaoxia Wang,[†] Xiaoli Zhu,[†] Changzeng Fan,[‡] Zongyin Yang,[§] Limin Tong,[§] Xiangfeng Duan,[∥] and Anlian Pan*[,†]

[†]Key Laboratory for Micro-Nano Physics and Technology of Hunan Province, State Key Laboratory of Chemo/Biosensing and Chemometrics, College of Physics and Microelectronics Science, Hunan University, Changsha 410082, China

[‡]State Key Laboratory of Metastable Materials Science and Technology, Yanshan University, Qinhuangdao 066004, China

[§]State Key Laboratory of Modern Optical Instrumentation, Department of Optical Engineering, Zhejiang University, Hangzhou 310027, China

[∥]Department of Chemistry and Biochemistry and California NanoSystems Institute, University of California at Los Angeles, Los Angeles, California 90095, United States

ABSTRACT: Compact wavelength-sensitive optical components are desirable for optical information processing and communication in photonic integrated system. In this work, optical waveguiding along single composition-graded CdS_xSe_{1-x} nanowires were systematically investigated. Under a focused laser excitation, the excited light can be guided passively along the bandgap-increased direction of the nanowire, keeping the photonic energy of the guided light almost unchanged during the whole propagation. In comparison, the excited light is guided actively through incessantly repeated band-to-band reabsorption and re-emitting processes along the bandgap-decreased direction, resulting in a gradual wavelength conversion during propagation. On the basis of this wavelength-converted waveguiding, a concept of nanoscale wavelength splitter is demonstrated by assembling a graded nanowire with several composition-uniform nanowires into branched nanowire structure. Our study indicates that composition-graded semiconductor nanowires would open new exciting opportunities in developing new wavelength-sensitive optical components for integrated nanophotonic devices.

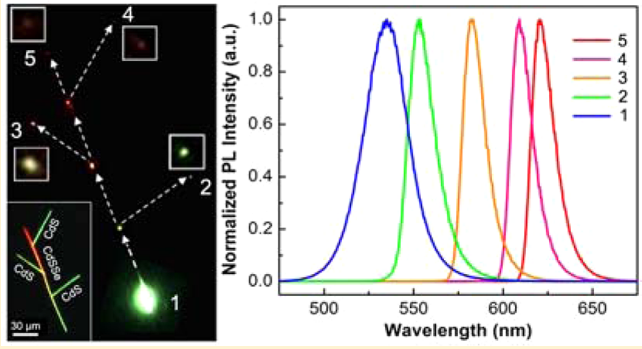

KEYWORDS: *Semiconductor nanowires, waveguiding, wavelength-selective, information devices, composition-graded*

Optical information processing and communication in an compact photonic integrated system calls for a development toward diverse nanoscale wavelength-sensitive optical devices and systems,[1−6] such as wavelength multiplexer,[7,8] wavelength converter,[9,10] photonic beam splitter[11] and wavelength-selective optical filter and waveguide.[12,13] In the past years, different structures, including photonic crystal,[4] diffraction grating,[14] dielectric-loaded plasmonic waveguide,[15] silicon-on-insulator waveguide[16,17] and so on have been proposed to design nanoscale wavelength-sensitive optical components.

Benefited from the unique one-dimensional footprint and versatile physical/chemical properties of semiconductor nanowires, developing semiconductor nanowire-based wavelength-sensitive optical devices would open new opportunities for integrated nanophotonics. At present, although semiconductor nanowires have been used as excellent nanoscale light source,[18−20] optical waveguiding cavity[21−23] as well as good candidates for realizing nanophotonic components and circuits,[24−28] nanowire-based wavelength-sensitive optical devices have rarely been investigated.[4,5]

In this work, nanoscale wavelength-selective optical waveguiding has been realized in single composition-graded CdS_xSe_{1-x} nanowires under locally optical excitation. These wires can function like a wavelength multiplexer when the excited light guides toward their wide bandgap end (WE), where the wavelength of the output signal is determined or selected by the excitation position along the length. On the other hand, the photon energy of the excited light will gradually decrease (wavelength increase) with increasing propagation distance during its guiding toward the narrow bandgap end (NE) of the wire. On the basis of this wavelength-converted waveguiding, a concept of nanoscale wavelength splitter is achieved through the branched nanowire structure composed

Received: July 20, 2012
Published: August 3, 2012

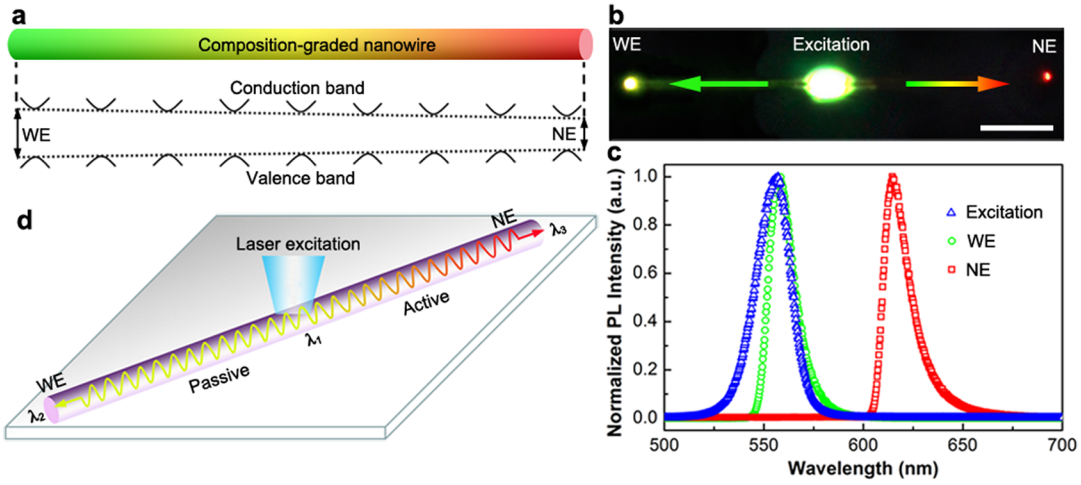

Figure 1. (a) Schematic diagram of a composition-graded nanowire and its graded bandgap structure along the axial direction. (b) Real-color PL image of a composition-graded nanowire under intermediately excited by a focused laser with a spot size of ~5 μm. Scale bar, 20 μm. (c) Normalized PL spectra of the emission from the original excitation position (blue), the left end (green), and the right end (red) of the nanowire waveguide. (d) Schematic waveguiding of the excited light along the two opposite directions. The emitted light is passively guided toward the WE and actively guided toward the NE of the wire, respectively.

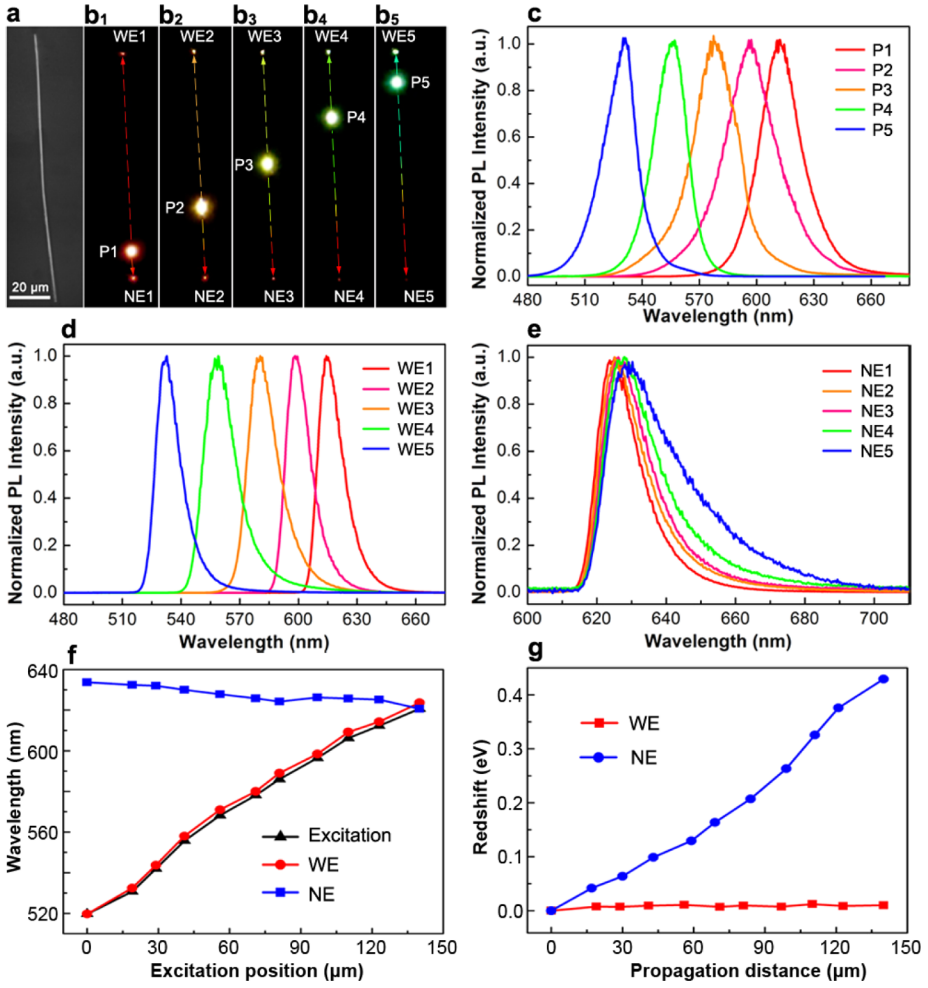

Figure 2. (a) SEM image of the examined composition-graded nanowire. (b_1–b_5) Real-color PL images of the wire locally excited in turn at different positions (P1–P5). (c–e) PL spectra collected at the excitation positions (P1–P5), the WE (WE1–WE5), and the NE (NE1–NE5) of the wire, respectively. (f) Plots of PL peak wavelength vs excitation position. The excitation position is defined by the distance from the WE to the excitation spot. (g) Propagation distance dependent spectral redshift of the detected output signals at the two opposite ends of the wire. The propagation distance is calculated from the excitation spot to the wire ends.

dx.doi.org/10.1021/nl302693c | *Nano Lett.* 2012, 12, 5003–5007

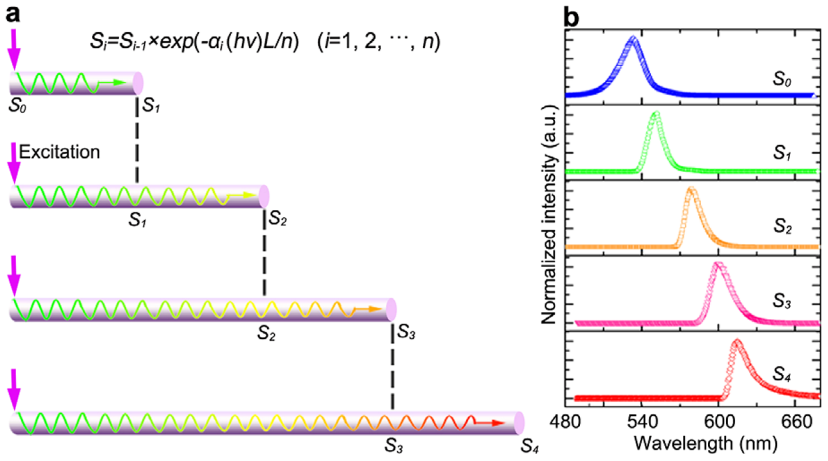

Figure 3. (a) Finite element model for calculating the transported PL spectra along the bandgap-decreased direction of the composition-graded nanowire by using semiconductor absorption rule. (b) Initial spectrum before guiding (S_0), and the representative simulated spectra at four different propagation distances (S_1–S_4), respectively. S_0 is given by the in situ PL spectrum of the excited light at the WE of the wire. During simulation, the nanowire is divided into n = 70 sections, L = 140 μm, $E_g(0)$ = 2.38 eV and $E_g(L)$ = 2.00 eV are the bandgap values of the materials at the WE and the NE, respectively.

of a composition-graded nanowire trunk and several composition-uniform nanowires branches.

The composition-graded CdS_xSe_{1-x} alloy nanowires, which possess a gradually tunable bandgap structure from one end to the other along their axial direction (schematically shown in Figure 1a), were synthesized via a thermal evaporation route with a moving source.[29] The maximum range of bandgap tunability along the length of these nanowires is from ~1.74 eV (NE, CdSe) up to ~2.42 eV (WE, CdS). Figures 1b shows the real-color photoluminescent (PL) photograph of a graded nanowire intermediately excited with a focused laser (Ar^+, 488 nm). We can see that a portion of the excited light is guided out of the both ends. However, the color at the NE changes from original green to red, while the color at the WE keeps the same as original green. This color difference is further confirmed by corresponding PL spectra in Figure 1c, which shows that the PL peak wavelength at the WE is almost the same as that at the excitation position (both ~560 nm), while the PL peak wavelength at the NE largely redshifts to ~615 nm. The exhibited different colors/peak wavelength of the guided light at the two ends indicates that the excited light has undergone different travel processes, which can be qualitatively explained by the graded bandgap structure along the length of the nanowire. As schematically shown in Figure 1d, the excited light (λ_1) at the excitation position can be passively propagated toward the WE since interband optical absorption cannot take place for the gradually increased bandgaps along the propagation direction. In this case, the nanowire cavity acts as an optically transparent medium and the excited light transmits along the wire mainly through total internal reflections, keeping the photonic energy of the guided light almost unchanged during the whole propagation ($\lambda_2 = \lambda_1$). While for the opposite direction, the excited light is guided actively through incessantly repeated band-to-band reabsorption and re-emitting processes due to the gradual-decreased bandgap along the propagation direction, resulting in the photonic energy gradually decreased (redshift) with increasing propagation distance ($\lambda_3 > \lambda_1$). As a result, the wavelength of the initial excited signal will finally convert into two different values at the two ends, as shown in Figures 1b,c. This special wavelength converted/selective waveguiding offers promising applications in designing nanoscale wavelength-sensitive optical devices.

For further investigation of the details of light propagation along these composition-graded nanowires, another representative nanowire is excited at several different positions in turn along its axial direction, and the output optical signals from its both ends are detected simultaneously on a confocal micro-PL system (WITec, alpha-300). This wire has a length of ~140 μm (Figure 2a) with bandedge emission spanning from ~520 to ~620 nm along its entire length. As shown in Figure $2b_1$–b_5, the emission color from the excitation position changes from red to green with the excitation position moved from P1 to P5 due to the gradually increased bandgap along the moving direction. This color transition is very consistent to the corresponding PL spectra in Figure 2c with their PL peak wavelengths changed from 530 to 612 nm accordingly. In addition, we can see that the excited light at all the positions can be guided back to back toward the two opposite directions and emitted at both ends. The color of the guided light at the WE (WE1–WE5) keeps the same as their respective excitation position (P1–P5), while the color at the NE (NE1–NE5) always exhibits red for all of the situations. The spectra shown in Figure 2d demonstrate that the guided lights at the WE exhibit very similar spectra to corresponding excitation positions, and the spectra of the optical signals from the NE for all the different excitations are largely overlapped (Figure 2e) with almost a same peak wavelength at around 630 nm.

The excitation position dependent peak wavelength (Figure 2f) further reveals that the excited light has been transported to the WE along the bandgap-increased direction without significant change of the wavelength. In this case, the composition-graded nanowire can function like a wavelength multiplexer with multi-input channels (excitation positions) and one output channel (WE). On the contrary, the excited lights at different positions all redshift to a constant value entered at around 630 nm when it reaches the NE after guiding along the bandgap-decreased direction. Additionally, the output wavelength is in very consistent with the emission wavelength of onsite material bandgap at the NE. All these results agree well with previously proposed optical waveguiding mechanism (Figure 1d). Figure 2g gives the propagation distance

dx.doi.org/10.1021/nl302693c | *Nano Lett.* 2012, 12, 5003–5007

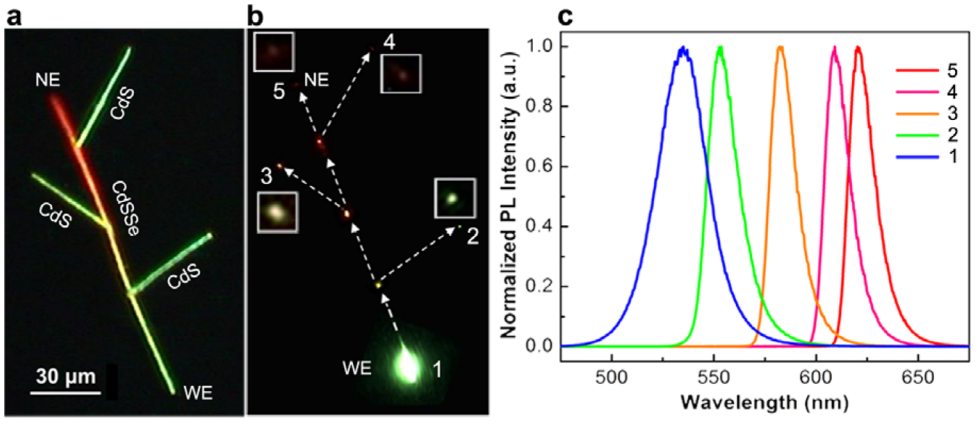

Figure 4. Real-color PL images of the nanowire branched structure under a diffused laser illumination (a) and focused excitation at the WE of the trunk (b), respectively. The excited light at the WE is guided into the three branches (2−4) and to the NE of the trunk (5), respectively. Insets, the magnified (×4) views of the output signals at the output ends 2−5, respectively. (c) The detected PL spectra at the positions 1−5 of indicated in panel b, respectively.

dependent spectral redshift of the excited light guided along the two opposite directions. The results more clearly reflect that the photonic energy of the excited light have total different redshift features along the two opposite guiding directions with a negligible redshift along the bandgap-increased direction and a maximum redshift up to 0.45 eV along the bandgap-decreased direction, respectively.

The wavelength conversion/redshift along the bandgap-decreased direction can be confirmed quantitatively using the finite element simulation based on the fundamental optical absorption theory of semiconductors.[30] During simulation, the graded wire with a length of L is divided into n sections (Figure 3a). As long as L/n is small enough, each section can be considered as a composition-homogeneous medium and the bandgap energy within i section, $E_g(i)$, is a constant value, which can be given as

$$E_g(i) = E_g(0) + \frac{E_g(L) - E_g(0)}{n} i \qquad (i = 0, 1, 2, \cdots, n) \tag{1}$$

where $E_g(0)$ and $E_g(L)$ correspond to the bandgap energy of the two ends, respectively. The spectrum S_i after transport i sections will be given by[30]

$$S_i = S_{i-1} e^{-\alpha_i(h\nu)L/n} \qquad (i = 1, 2, 3, \cdots, n) \tag{2}$$

where $\alpha_i(h\nu)$ is the absorption coefficient within i section, which can be defined by the following equations for different energy scale:[31]

$$\text{For } E > E_g(i), \qquad \alpha_i(h\nu) = A_0\sqrt{E - E_g(i)} \tag{3}$$

$$\text{For } E \le E_g(i), \qquad \alpha_i(h\nu) = A_0\sqrt{\frac{kT}{2\sigma(i)}}\exp\left[\frac{\sigma(i)}{kT}\left(E - E_g(i) - \frac{kT}{2\sigma(i)}\right)\right] \tag{4}$$

where $A_0 = 2.0 \times 10^4$ cm^{-1}·eV$^{-1/2}$, $kT = 25$ meV is the thermal energy at room temperature, h is Planck's constant, ν is the photon frequency, $\sigma(i)$ is the dimensionless phenomenological fitting parameter within the i section of the graded wire, which behaves as[32]

$$\sigma(i) = \sigma_0(i)\frac{2kT}{\hbar\omega_0(i)}\tanh\left(\frac{\hbar\omega_0(i)}{2kT}\right) \tag{5}$$

here, $\sigma_0(i)$ and $\omega_0(i)$ changes gradually with the composition variation along the entire length of the wire, and they are composition dependent in the follow manner

$$\sigma_0(i) = \sigma_{0(\text{cds})} \times x(i) + \sigma_{0(\text{cdse})} \times [1 - x(i)] \tag{6}$$

$$\hbar\omega_0(i) = \hbar\omega_{0(\text{CdS})} \times x(i) + \hbar\omega_{0(\text{CdSe})} \times [1 - x(i)] \tag{7}$$

where $\sigma_{0(\text{CdS})} = 2.8$ eV, $\sigma_{0(\text{CdSe})} = 2.3$ eV, $\hbar\omega_{0(\text{CdS})} = 38$ meV, $\hbar\omega_{0(\text{CdS})} = 27$ meV,[33] and $x(i)$ is the mole fraction of S element within the i section, which can be calculated from

$$E_g(i) = E_{g(\text{CdS})} \times x(i) + E_{g(\text{CdSe})}[1 - x(i)] \tag{8}$$

where $E_{g(\text{CdS})} = 2.42$ eV and $E_{g(\text{CdSe})} = 1.74$ eV is the room temperature bandgap of CdS and CdSe, respectively. Considering the wire in Figure 2 and using the eqs 1−8, the spectra after different propagation distances are calculated. As shown in Figure 3b, the peak wavelength of the obtained spectra largely shift to the low energy region with increasing the propagation distance, which confirms that the observed wavelength converted waveguiding definitely originates from the gradually decreased bandgap structure.

This propagation distance-dependent wavelength-converted waveguiding makes composition-graded nanowires have potential applications in designing nanoscale wavelength-sensitive optical devices. As a representative, here we demonstrate the realization of wavelength-selective waveguiding (wavelength splitter) using a branched nanowire structure with a composition-graded nanowire as the backbone. The construction of the branched nanowire structure was carried out under an optical microscope (Zeiss, Imager.A2) equipped with a superlong-working distance objective. Using homemade fiber probes (drawn from a standard single-mode optical fiber (Corning, SMF-28)) for micromanipulation,[20] dispersed nanowires on a substrate can be rationally assembled into a branched structure. Figure 4a is the real-color PL image of a representative branched structure under diffused laser illumination. This branched structure consists of three composition-uniform CdS nanowire branches and a composition-graded CdS_xSe_{1-x} nanowire trunk with the roots of each branch physically touched at different positions of the graded

dx.doi.org/10.1021/nl302693c | Nano Lett. 2012, 12, 5003−5007

nanowire trunk. Figure 4b shows the corresponding far-field PL image of the branched structure with a focused laser excited at the WE of the trunk (see the bright green light spot in position 1). As can be seen, the emitted light has been guided to the NE of the graded nanowire, where the emission color has changed into red (see the weak red light spot in position 5). Meanwhile, light spot with different color is observed at each end of the branches (position 2−4), and the exhibited color keeps the same as that of corresponding junction, which indicates the guided light within the trunk has been selectively guided out of the branches. Figure 4c plots the normalized PL spectra detected at the input end (spectrum 1) and all output ends (spectrum 2−5). We can see all the spectra from branches (spectrum 2−4) locate between the spectrum at the WE (spectrum 1) and NE (spectrum 5) of the graded trunk, with peak wavelength increases from branch 2 to branch 4, which further quantitatively demonstrate that all the branches guide out light with different wavelengths from the trunk. As previously discussed, the guided light within the composition graded nanowire trunk, possesses continuously converted wavelengths during its guiding toward the NE. The guided light can partially transmit into the branches through side-by-side coupling[1] at each junction and then passively transport along the branches, in which further wavelength change is negligible since the CdS nanowire branches have a relatively larger bandgap than that of any positions in the graded nanowire trunk.

In summary, optical transport properties of composition-graded CdS_xSe_{1-x} nanowires were investigated systematically. When the wires are excited intermediately by a focused laser, the emitted light can transport back to back along the length and output at both ends. The output wavelength at the wide bandgap end remains the same as the emission wavelength at the excitation position, making these wires function like a wavelength multiplexer. In comparison, the excited light undergoes a gradual wavelength conversion during the propagation toward the narrow bandgap end, and finally outputs with a wavelength value related to the material bandgap at this end. Theoretical simulation further reveals that this wavelength-converted waveguiding originates from the gradually decreased bandgap induced band-to-band reabsorption and re-emission processes. More importantly, based on this wavelength-converted waveguiding, a concept of nanowire-based wavelength splitter is achieved by assembling a graded nanowire with several composition-uniform nanowires into branched nanowire structure. Our study represents significant progress toward the development of nanowire-based optical information components for all-optical processing in integrated nanophotonics.

AUTHOR INFORMATION

Corresponding Author

*E-mail: anlian.pan@hnu.edu.cn.

Author Contributions

⊥These authors contributed equally.

Notes

The authors declare no competing financial interest.

ACKNOWLEDGMENTS

The authors are grateful to the NSF of China (Nos. 90923014 and 10974050), the National Basic Research Program of China (No. 2012CB932703), the Research Fund for the Doctoral Program of Higher Education (No. 20110161110034), and the Aid Program for Science and Technology Innovative Research Team in Higher Educational Institutions of Hunan Province for financial support.

REFERENCES

(1) Law, M.; Sirbuly, D.; Johnson, J.; Goldberger, J.; Saykally, R.; Yang, P. *Science* **2004**, *305*, 1269.
(2) Qian, F.; Li, Y.; Gradečak, S.; Park, H. G.; Dong, Y.; Ding, Y.; Wang, Z. L.; Lieber, C. M. *Nat. Mater.* **2008**, *7*, 701.
(3) Huang, Y.; Duan, X. F.; Lieber, C. M. *Small* **2005**, *1*, 142.
(4) Park, H. G.; Barrelet, C. J.; Wu, Y. N.; Tian, B. Z.; Qian, F.; Lieber, C. M. *Nat. Photonics* **2008**, *2*, 622.
(5) Skirtach, A. G.; Karageorgiev, P.; De Geest, B. G.; Pazos-Perez, N.; Braun, D.; Sukhorukov, G. B. *Adv. Mater.* **2008**, *20*, 506.
(6) Yan, H.; Choe, H. S.; Nam, S. W.; Hu, Y. J.; Das, S.; Klemic, J. F.; Ellenbogen, J. C.; Lieber, C. M. *Nature* **2011**, *470*, 240.
(7) Psaltis, D. *Science* **2002**, *298*, 1359.
(8) Foster, M. A.; Turner, A. C.; Sharping, J. E.; Schmidt, B. S.; Lipson, M.; Gaeta, A. L. *Nature* **2006**, *441*, 960.
(9) Raghunathan, V.; Claps, R.; Dimitropoulos, D.; Jalali, B. *Appl. Phys. Lett.* **2004**, *85*, 34.
(10) Matsuura, M.; Raz, O.; Gomez-Agis, F.; Calabretta, N.; Dorren, H. J. S. *Opt. Express* **2011**, *19*, 551.
(11) Xing, X. B.; Zhu, H.; Wang, Y. Q.; Li, B. J. *Nano Lett.* **2008**, *8*, 2839.
(12) Dainese, M.; Swillo, M.; Wosinski, L.; Thylen, L. *Opt. Commun.* **2006**, *260*, 514.
(13) Chiu, H. K.; Chang, C. H.; Hou, C. H.; Chen, C. C.; Lee, C. C. *Appl. Opt.* **2011**, *50*, 227.
(14) Taylor, H. F. *Opt. Commun.* **1973**, *8*, 421.
(15) Chen, Z.; Holmgaard, T.; Bozhevolnyi, S. I.; Krasavin, A. V.; Zayats, A. V.; Markey, L.; Dereux, A. *Opt. Lett.* **2009**, *34*, 310.
(16) Yamada, H.; Chu, T.; Ishida, S.; Arakawa, Y. *Proc. of SPIE* **2005**, 60192X-1.
(17) Dai, D.; He, S. *Proc. of SPIE* **2009**, 72200D.
(18) Qian, F.; Gradecak, S.; Li, Y.; Wen, C. Y.; Lieber, C. M. *Nano Lett.* **2005**, *5*, 2287.
(19) Yang, Z. Y.; Xu, J. Y.; Wang, P.; Zhuang, X. J.; Pan, A. L.; Tong, L. M. *Nano Lett.* **2011**, *11*, 5085.
(20) Pan, A. L.; Yang, H.; Liu, R. B.; Yu, R. C.; Zou, B. S.; Wang, Z. L. *J. Am. Chem. Soc.* **2005**, *127*, 15692.
(21) Pan, A. L.; Liu, D.; Liu, R. B.; Wang, F. F.; Zhu, X.; Zou, B. S. *Small* **2005**, *1*, 980.
(22) Yan, R. X.; Pausauskie, P.; Huang, J. X.; Yang, P. D. *Proc. Natl. Acad. Sci. U.S.A.* **2009**, *106*, 21045.
(23) Piccione, B.; van Vugt, L. K.; Agarwal, R. *Nano Lett.* **2010**, *10*, 2251.
(24) Duan, X. F.; Huang, Y.; Agarwal, R.; Lieber, C. M. *Nature* **2003**, *421*, 241.
(25) Wang, Z. L.; Song, J. H. *Science* **2006**, *312*, 242.
(26) Zhuang, X. J.; Ning, C. Z.; Pan, A. L. *Adv. Mater.* **2011**, *24*, 13.
(27) Huang, Y.; Duan, X. F.; Cui, Y.; Lauhon, L. J.; Kim, K. H.; Lieber, C. M. *Science* **2001**, *294*, 1313.
(28) Barrelet, C. J.; Greytak, A. B.; Lieber, C. M. *Nano Lett.* **2004**, *4*, 1981.
(29) Gu, F. X.; Yang, Z. Y.; Yu, H. K.; Xu, J. Y.; Wang, P.; Tong, L. M.; Pan, A. L. *J. Am. Chem. Soc.* **2011**, *133*, 2037.
(30) Pan, A. L.; Wang, X.; He, P. B.; Zhang, Q. L.; Wan, Q.; Zacharias, M.; Zhu, X.; Zou, B. S. *Nano Lett.* **2007**, *7*, 2970.
(31) Urbach, F. *Phys. Rev.* **1953**, *92*, 1324.
(32) Mahr, H. *Phys. Rev.* **1962**, *125*, 1510.
(33) Samuel, L.; Brada, Y.; Beserman, R. *Phys. Rev. B* **1988**, *37*, 4671.